AJNR

MRI of optic chiasm and optic pathways.

A Albert, B C Lee, L Saint-Louis and M D Deck

AJNR Am J Neuroradiol 1986, 7 (2) 255-258
http://www.ajnr.org/content/7/2/255

MRI of Optic Chiasm and Optic Pathways

Ana Albert[1]
Benjamin C. P. Lee[1,2]
Leslie Saint-Louis[1]
Michael D. F. Deck[1]

Eight verified lesions of the optic chiasm were examined on 0.5 T magnetic resonance (MR) and GE 9800, 8800 computed tomographic (CT) scanners. Enlargement of the optic chiasm was demonstrated in all cases. There was some change of MR signal compared with brain in all but one case, which had no resemblance to contrast enhancement on CT scans. The signal was specific for hematoma in one case. Abnormal signal, probably signifying tumor spread into the optic radiation, was detected on T2-weighted images in one case. The resolution of MR scans is similar or superior to CT, and sagittal views are most useful in evaluating lesions in this location.

Abnormalities of the optic chiasm are difficult to detect on CT scans because of the poor contrast difference between this structure and the subarachnoid space and the frequent occurrence of streak artifacts in this region [1–4]. Primary lesions are seldom distinguishable from secondary involvement by adjacent pathology. Metrizamide CT is usually performed for detailed delineation of lesions in this location [5]. High-resolution MR scanning is reported to be helpful in evaluating the normal optic chiasm and nerves, but documentation of pathologic lesions is limited [6]. Our study was aimed at comparing MR with plain CT and metrizamide CT in the evaluation of lesions of the optic chiasm, tracts, and radiation.

Subjects and Methods

Eight patients with lesions of the optic chiasm were examined: Three had primary optic chiasm tumors, two had extensions of optic nerve gliomas posteriorly into the optic chiasm and tract, one had a hematoma (probably secondary to a glioma), one had infiltration by an incompletely excised craniopharyngioma, and one had intracranial extension of retinoblastoma. Spin-echo (SE) MR scanning was performed on a 0.5 T superconducting scanner: Single- or multisection scans in the axial and sagittal planes were obtained in all cases using echo times (TEs) of 30 msec, repetition times (TRs) of 500 msec (SE 30/500), T1-weighted technique, and TE 90, TR 1500 (SE 90/1500), T2-weighted technique, in all cases. Supplementary coronal sections and SE imaging using multiecho (SE 30–120/2000) and inversion-recovery techniques were used in selected cases. Multisection scans were 8 mm; single sections were 10 mm thick. Two signal averages were used in all scanning sequences. Spatial resolution was 1.2–1.5 mm.

CT was performed using GE 8800, 9800, or equivalent third- or fourth-generation scanners: 1.5–3-mm-thick axial or coronal sections were obtained after a single dose of intravenous contrast material in all cases. Metrizamide CT using 1.5 mm axial sections with multiple-plane reconstruction was performed in two cases.

Results

The optic chiasms were enlarged in all five cases of glioma: symmetric in three and asymmetric in two (figs. 1 and 2). There was extension into the optic tract in two, with compression of the ambient cistern, and displacement of the midbrain in

Received February 12, 1985; accepted after revision August 14, 1985.

[1]Department of Radiology, Cornell University Medical College, New York City, NY 10021.

[2]Present address: Department of Radiology, University of California, Davis, Medical Center, 4301 X St., Sacramento, CA 95817. Address reprint requests to B. C. P. Lee.

***AJNR* 7:255–258, March/April 1986**
0195-6108/86/0702-0255

A B

Fig. 1.—Glioma, clinical diagnosis. SE 30/500 images. **A**, 2-year-old patient, sagittal view. Enlarged optic chiasm and nerve (*arrowheads*). **B**, 21-year-old patient, axial view. Symmetric enlargement of optic chiasm (*arrowheads*).

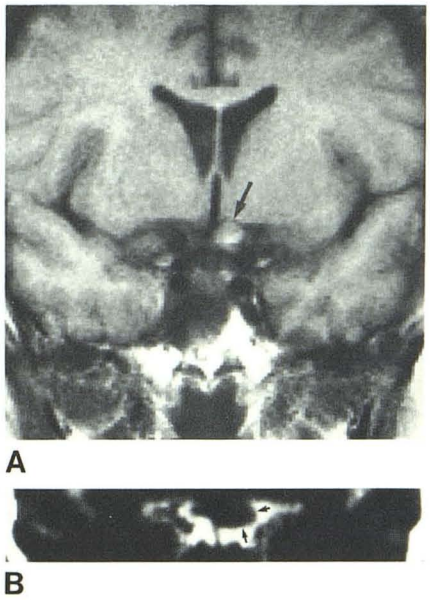

A B

Fig. 2.—Glioma, 21-year-old patient, surgical pathology. **A,** Coronal SE 30/500 image. Asymmetric enlargement of optic chiasm (*arrow*). **B,** Coronal reformatted metrizamide CT scan confirms enlargement (*arrows*).

Fig. 3.—Glioma, 10-year-old patient, surgical pathology. Axial SE 30/500 image. Optic chiasm glioma with extension into optic tract (*arrowheads*) causing some compression of midbrain.

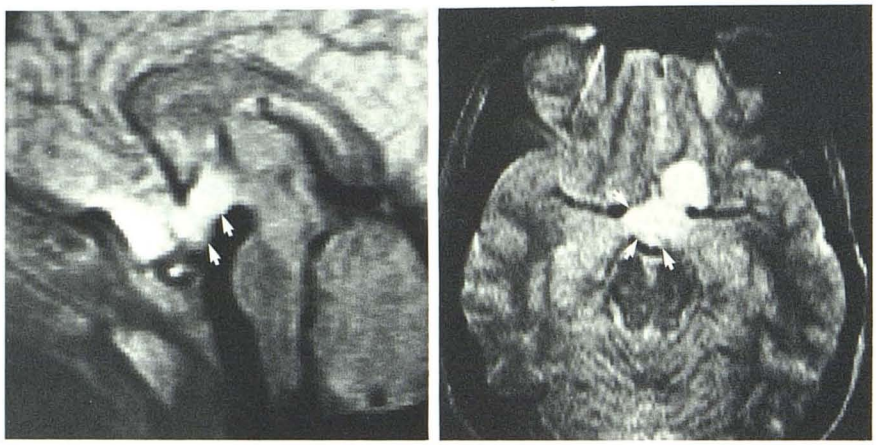

A B

Fig. 4.—Glioma, 20-year-old patient, surgical pathology. SE 90/1500 images. Sagittal (**A**) and axial (**B**) views. Increased signal of enlarged optic chiasm (*arrows*) with involvement of optic nerves.

one case (fig. 3). The lesions were isointense with brain on T1-weighted (SE 30/500) techniques in four cases, becoming hyperintense on T2-weighted (SE 90/1500) techniques (fig. 4). One case was hypointense on T1-weighted (SE 30/500) and hyperintense on T2-weighted images. Hyperintense signal in the occipital radiation, presumably the result of extension of the glioma, was shown in one case (fig. 5). One lesion was hyperintense on both T1 and T2 imaging techniques (fig. 6) because of a hematoma that was surgically verified.

Enlargement of the optic chiasm was seen in the cases of retinoblastoma and postoperative craniopharyngioma (fig. 7). The signal of the latter was isointense in all imaging sequences. Retinoblastoma was isointense on T1 (SE 30/500) and hyperintense on T2 (SE 90/1500) techniques.

CT scans were abnormal in all cases: the optic chiasm was enlarged in six cases; large suprasellar masses inseparable

Fig. 5.—Glioma, 10-year-old patient, clinical diagnosis. SE 90/1500 sagittal view. Increased signal in optic tract (*arrows*) and radiation (*arrowhead*).

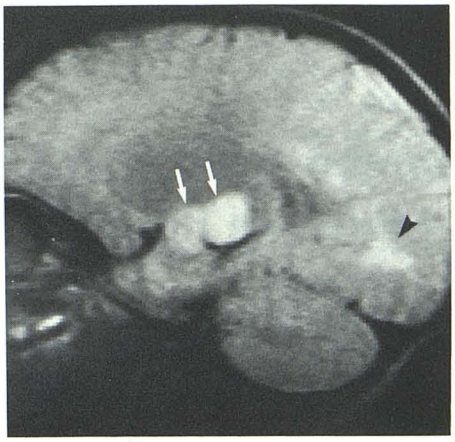

5

Fig. 6.—Hematoma, 37-year-old patient, surgical pathology. SE 30/500 sagittal image. Increased signal in optic chiasm. (Signal was unchanged on SE 90/1500 image.)

6

A

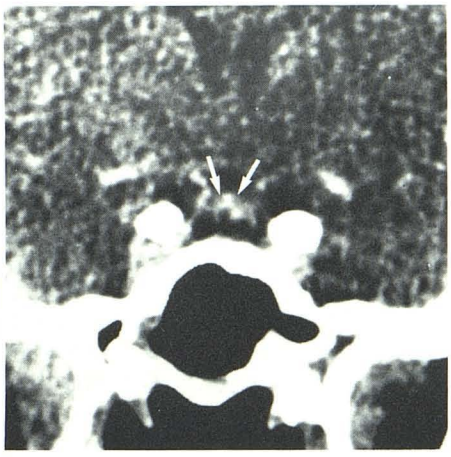

B

C

Fig. 7.—Postoperative residual craniopharyngioma, 15-year-old patient, surgical pathology. **A**, SE 30/500 sagittal image. Enlarged optic chiasm (*arrow*). **B**, Coronal contrast-enhanced CT scan. Irregular optic chiasm (*arrows*). **C**, Sagittal reformatted metrizamide CT scan confirms enlargement (*arrow*).

from the chiasm were seen in two cases. Three cases had contrast enhancement. Extension of tumor beyond the optic tract was not demonstrated.

Discussion

Technique

The spatial resolution of MR images is dependent on the matrix size, contrast between the optic chiasm and subarachnoid space, thickness of the sections, and the signal-to-noise (S/N) ratio [7–9]. The matrix size may be decreased by using a greater number of gradient steps, which unfortunately results in some decrease in the contrast. The sections may be made very thin, at the expense of decreased S/N, which has to be compensated by increasing the number of signal averages. At the magnetic field used in our study, it was found that a slice thickness of 8 mm using two signal averages is adequate for demonstration of the optic chiasm. Thinner sections required unacceptably long scanning times. The optimal technique for anatomic evaluation is SE 30/500, which in addition provides some T1 data.

The optimal plane for MR scanning depends on the precise location of the lesions. The midline sagittal view provides the most sensitive evaluation of changes in size of the chiasm and intracranial parts of the optic nerves. Coronal views are best for evaluating eccentrically situated lesions. Axial views are optimal for examining retrochiasmal spread in the optic tract and radiation. Off-lateral sagittal views may be used to supplement the other views. Spatial resolution is very similar to that of metrizamide CT.

Lesions of the optic tract are poorly seen on CT scans unless there is contrast enhancement and pronounced compression of the brainstem. The extent of such involvement is shown well on axial MR.

Contrast

The signal characteristics of lesions using different imaging sequences are sometimes helpful in suggesting the compo-

nents of optic chiasm lesions. The increased signal in all imaging sequences in one case suggested that the lesion had contents with short T1 and long T2 relaxation times, which are frequently seen with hematoma or fat [10]. The normal appearance of the CT scan without an area of fat density is compatible with hematoma, which was proved at surgical exploration.

In the other cases the normal or slightly decreased signal of the lesion on T1-weighted (SE 30/500) and increased signal on T2-weighted (SE 90/1500) images is nonspecific and is caused by tumor infiltration or edema. The TE used in T2-weighted techniques is sometimes critical in differentiating tumor tissue from signal of cerebrospinal fluid (CSF): In one case tumor tissue had brighter signal than CSF when TE 90 was used, but the signal intensities were identical when this was increased to TE 120.

The abnormal signal on T2-weighted MR images bears little resemblance to contrast enhancement on CT scans. The margins of abnormal MR signal were usually poorly defined, but the number of cases studied was too small to make a judgment as to the malignant or benign nature of the lesions based on the appearance of the MR margins. The ability to detect contrast changes in the optic pathways when CT failed to show altered attenuation is excellent at the magnetic field strength used in this study. The superior spatial and contrast sensitivity of MR may be helpful in determining extent of disease and suitability for surgical or radiation therapy [11].

REFERENCES

1. Daniels DL, Haughton VM, Williams AL, Gager WE, Berns TF. Computed tomography of the optic chiasm. *Radiology* **1983;**137:123–127
2. Taylor S. High resolution computed tomography of the sella. *Radiol Clin North Am* **1982;**20:207–236
3. Maravilla KR, Kirks DR, Maravilla AM, Diehl JT. CT in the evaluation of sellar and parasellar lesions: the value of sagittal and coronal reconstruction. *Comput Radiol* **1978;**2:237–249
4. Cohen WA, Pinto RS, Kricheff II. Dynamic CT scanning for visualization of the parasellar cortical arteries. *AJR* **1982;**27:905–909
5. Drayer BP, Rosenbaum AE, Kennerdell JS, Robinson AG, Bank WO, Deeb ZL. Computed tomographic diagnosis of suprasellar masses by intrathecal enhancement. *Radiology* **1977;**123:339–344
6. Daniels DL, Herfkins R, Gager WE, et al. Magnetic resonance imaging of the optic nerves and chiasm. *Radiology* **1984;**152:79–83
7. Wehrli FW, MacFall J, Newton TH. Parameters determining the appearance of NMR images. In: Newton TH, Potts DG, eds. *Modern neuroradiology*, vol 2. *Advanced imaging techniques.* Clavadel Press, San Anselmo, CA: Clavadel, **1983**:81–118
8. Crooks LE, Mills CM, Davis PL, et al. Visualization of cerebral and vascular abnormalities by NMR imaging. The effects of imaging parameters on contrast. *Radiology* **1982;**144:843–852
9. Kneeland JB, Knowles RJR, Cahill PT. Magnetic resonance imaging systems: optimization in clinical use. *Radiology* **1984;**153:473–478
10. Bottomley PA, Foster TH, Raymond E, et al. A review of normal tissue hydrogen NMR relaxation times and relaxation mechanisms from 1–100 MHz: Dependence on tissue type, NMR frequency, temperature, species, excision and age. *Med Phys* **1984;**11:425–448
11. Edelstein WA, Bottomley PA, Hart HR, Smith LS. Signal, noise and contrast in nuclear magnetic resonance (NMR) imaging. *J Comput Assist Tomogr* **1983;**7:391–401